Core/Shell pH-Sensitive Micelles Self-Assembled from Cholesterol Conjugated Oligopeptides for Anticancer Drug Delivery

Xin Dong Guo, Li Juan Zhang, Yun Chen, and Yu Qian
School of Chemistry and Chemical Engineering, South China University of Technology, Guangzhou 510640, P. R. China

DOI 10.1002/aic.12119
Published online November 18, 2009 in Wiley InterScience (www.interscience.wiley.com).

A doxorubicin (DOX) delivery system of pH-sensitive micelles self-assembled from cholesterol conjugated His_5Arg_{10} (HR15-Chol) and $His_{10}Arg_{10}$ (HR20-Chol) has been described in this article. The amphiphilic molecules have low critical micelle concentrations of 17.8 and 28.2 μg/mL for HR15-Chol and HR20-Chol, respectively, even at a low pH of 5.0. The pH-sensitive histidine segment of the polypeptide block is insoluble at pH 7.4 but becomes positively charged and soluble via protonation at pH lower than 6.0. The size and zeta potential of DOX-loaded micelles increases with the decrease in pH. Coarse-grained simulations were performed to verify the structure of DOX-loaded micelles and pH sensitivity of HR15/20-Chol. The in vitro DOX release from the micelles is significantly accelerated by decreasing pH from 7.4 to 5.0. Furthermore, DOX release from the micelles is controlled by a Fickian diffusion mechanism. These micelles have great potential applications in delivering hydrophobic anticancer drugs for improved cancer therapy. © 2009 American Institute of Chemical Engineers *AIChE J,* 56: 1922–1931, 2010

Keywords: micelle, drug delivery, modelling, cholesterol, oligopeptide

Introduction

In the recent years, many new chemotherapeutic compounds have been developed for cancer therapy.[1–4] However, there are still various challenges for anticancer agent formulations which are often associated with their solubility, stability, sensitivity, and toxicity.[5,6] Recently, the novel drug delivery approaches have been investigated to obtain higher antitumor efficiency with reduced toxicity by altering the biodistribution of anticancer drugs, such as nanoparticles,[7–11] liquid emulsion,[12] and liposomes.[5] Compared to these systems, polymeric micelles hold a significant potential as drug delivery vesicles for a wide array of anticancer drugs due to their unique properties, such as high solubility, high drug loading capacity, and low toxicity.[13–18] It is well known that micelles have core/shell architecture that is composed of hydrophobic segments as internal core, providing a loading space for hydrophobic drugs, and hydrophilic segments as surrounding corona in aqueous medium, affecting the drug release behaviors.[19–21] Especially, the environmentally sensitive micelles were investigated as smart drug delivery systems for cancer therapy.[22–28] For example, Bae's group has developed a pH-sensitive carrier micelle self-assembled from poly(His-*co*-Phe)-*b*-poly(ethylene glycol) and poly(L-lactic acid)-*b*-poly(ethylene glycol).[14] These micelles showed noticeable pH-dependent behavior, leading to a quick release at pH 5.5 and a slow release at pH 7.4. However, one common problem for these micelles is their slow cellular internalization and lysosomal sequestration. The cellular uptake of these micelles is generally slow due to the steric repulsion of poly(ethylene glycol) (PEG) layers. Furthermore, these micelles are retained in several cytoplasmic organelles mainly lysosomes after internalized. Although pH-sensitive

Additional Supporting Information may be found in the online version of this article.

Correspondence concerning this article should be addressed to Y. Qian at ceyuqian@scut.edu.cn.

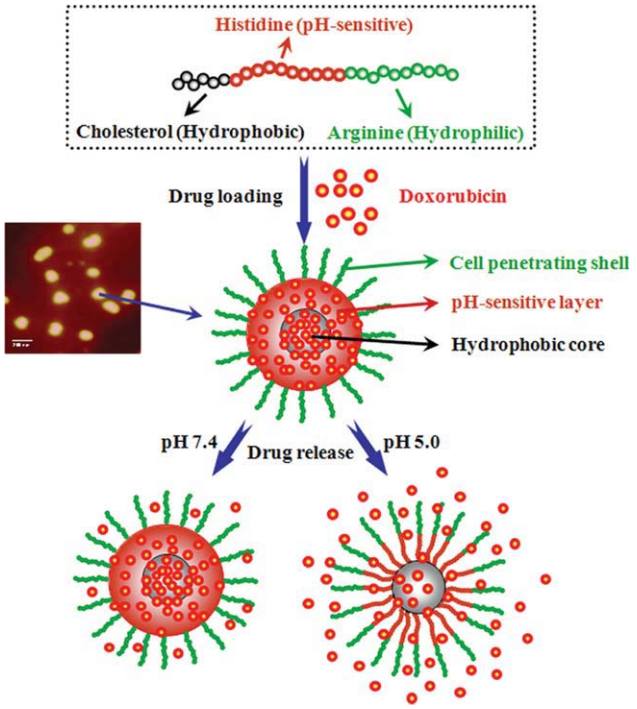

Scheme 1. Fabrication of DOX-loaded pH-sensitive cholesterol conjugated peptides micelles via self-assembly.

[Color figure can be viewed in the online issue, which is available at www.interscience.wiley.com.]

micelles have been extensively studied, it is still highly demanded to design carriers which can control the drug releasing rate at different pH environments.

Compared with the normal physiological environment of pH 7.4, the extracellular pH values in tumorous tissues are determined to be around 6.5–7.0,[29] and the lysosomal environment is typically acidic (pH 5.0).[30,31] Therefore, an ideal anticancer drug carrier should retain the drug at pH 7.4 and can quickly release it at a relatively lower pH (e.g., pH 5.0). In addition, the intracellular delivery could be facilitated by pH-sensitive pore-forming peptides,[32] cell penetrating peptides,[33,34] and synthetic endosomolytic polymers.[35] To get the endosomolytic polymers, the histidine residues can be introduced to provide imidazole groups. The imidazole group can be partially protonated at physiological pH conditions but served as a proton sponge in the lysosomal environment.[36,37]

In this work, the primary objective was to design pH-sensitive micelles which can escape releasing of drug in a normal physiological environment (pH 7.4) and destabilized at an early endosomal pH of 6.0. Following intravenous or intratumoral administration, the doxorubicin (DOX) loaded micelles are taken up to cells via endocytosis. As shown in Scheme 1, cholesterol, which is an essential constituent in mammalian cell membranes,[38] is selected as the hydrophobic core for carrying drugs and cell-penetrating arginine residues[39] as the outer layer. The histidine residues distribute in the middle layer, acting as a pH-sensitive part. The histidine layer is hydrophobic at the physiological environment (pH 7.4) to prevent the release of hydrophobic drugs. However, it converses to ionized hydrophilic ones by protonation of imidazole groups once internalized and transferred to a lysosome (pH 5.0), leading to the faster release of hydropholic drugs. DOX, a widely used anticancer drug, was selected as the model drug. The physicochemical properties of DOX-loaded micelles were examined by a variety of experimental techniques, such as particle size, zeta potential, SEM, etc.

Experimental Section

Materials

Cholesteryl chloroformate, anhydrous *N,N*-dimethylformamide (DMF), dimethyl sulfoxide (DMSO), *N,N*-dimethylacetamide (DMAC), and DOX hydrochloride were all purchased from Sigma-Aldrich and used as received. Triethylamine (TEA, $\geq$99%) from Sigma-Aldrich was further purified and distilled before use. Ultra pure water of high performance liquid chromatography (HPLC) grade was obtained from J.T. Baker. Phosphate-buffered saline (PBS) buffers were purchased from 1st BASE (Malaysia) and diluted to the intended concentration before use. Dulbecco's modified eagle media (DMEM) and Roswell Park Memorial Institute (RPMI) 1640 growth media, fetal bovine serum (FBS), penicillin, and streptomycin were all purchased from Invitrogen. 4T1 cell lines were obtained from ATCC and grown under the recommended conditions according to the supplier. The peptides, H_5R_{10} (HR15) and $H_{10}R_{10}$ (HR20), were designed by us and synthesized by GL Biochem (Shanghai, P. R. China) at more than 95% purity.

Conjugation of cholesterol onto the peptides

Scheme S1 (Supporting Information) illustrates the synthesis workflow and the structure of cholesterol conjugated peptides. TEA was purified using toluene sulphonyl chloride via distillation to remove any primary and secondary amines present. The purified TEA was then further distilled using sodium. In particular, HR15 (20 mg) was dissolved in anhydrous DMF (1.5 mL) and placed into a round bottom flask (50 mL) under argon. The purified TEA (18 μL) was subsequently added and stirred homogenously for 15 min under argon. Cholesteryl chloroformate (40 mg) was dissolved in anhydrous DMF (3.5 mL), and it was then slowly added dropwise into the solution of TEA and HR15. The molar ratio of TEA to cholesterol chloroformate to peptide was 15:10:1. The reaction was stirred for 48 h at room temperature (about 22°C) under argon. The crude product was centrifuged at 14,000 rpm to remove any by-products present and the supernatant was taken out. It was then dialyzed against DMF using a molecular weight cut-off (MWCO) of 1 kDa (Spectrum Laboratories) for 2 days, followed by dialysis against de-ionized (DI) water for another two more days. The conjugated peptide, HR15-Chol was harvested by freeze-drying.

Matrix-assisted laser desorption/ionization time of flight mass spectrometry

Successful conjugation of cholesterol onto the peptides was confirmed via matrix-assisted laser desorption/ionization time of flight (MALDI-TOF) mass spectrometry (Autoflex II, Bruker Daltronics). Briefly, peptides and conjugates were dissolved in DI water to a concentration of 100 mg/L. The solution was then mixed with α-cyano-4-hydroxycinnamic

acid matrix at a volumetric ratio of 1:5, about 0.5 μL of which were placed onto a ground steel plate spot. The theoretical molecular weights of HR15-Chol and HR20-Chol were 2677.19 kDa and 3362.86 kDa respectively, which appeared in MALDI-TOF mass spectra of these peptides (Figure S1 in Supporting Information), indicating the successful synthesis of the peptides. From the integration of cholesterol conjugated peptide and unmodified peptide peak areas, the grafting degree of cholesterol was estimated to be about 85%.

CMC measurement

The critical micelle concentration (CMC) of peptides was estimated by fluorescence spectroscopy using pyrene as a probe. Briefly, a series of peptide solutions containing 0.616 μM pyrene were prepared at various concentrations (0–1.28 mg/mL) in PBS buffer (pH 5.0, 6.0, 6.5, or 7.4, 20 mM). Excitation spectra of solutions were recorded from 300 to 360 nm at room temperature, with an emission wavelength of 395 nm and bandwidth of 1 nm, using a spectrofluorometer (Fluorolog® LFI 3751; Jobin Yvon Horiba, Edison, NY). The intensity ratios of I_{339} to I_{334} were plotted as a function of logarithm of peptide concentration. The CMC value was taken from the intersection of the tangent to the curve at the inflection with the horizontal tangent through the points at low concentrations. Take the CMC value of HR15/20-Chol at pH 5.0 as an example, the calculated results can be found from Figure S2 (Supporting Information).

Preparation of DOX-loaded micelles

DOX-loaded micelles were prepared by a membrane dialysis technique. Briefly, 5 mg DOX–HCl and 10 mg peptides were dissolved in 2 mL DMAC solvent. One drop of TEA (ca. 0.01 mL) was added to the solution to remove hydrochloride. The resulted solution was dropped into 10 mL DI water (filtered) under sonication for 10 min. The mixed solution was dialyzed against 1 L of DI water for 48 h at 20°C to using a dialysis bag with MWCO of 1000 Da (Spectra/Por 7; Spectrum Laboratories). The DI water was changed every 3 h for the first 12 h and once again the next day. After dialysis, the DOX-loaded micelles were filtered and harvested by freeze-drying.

Characterization of DOX-loaded micelles

The final DOX loading content in the peptides micelles was analyzed by an ultraviolet-visible spectrometer (UV-vis; Unico UV2450). Briefly, 1 mg of DOX loaded micelles was dissolved in 3 mL of DMSO, the micelles were broken up and the DOX was dissolved in the solution. The characteristic absorption of DOX at 481 nm was recorded and compared with a standard curve generated from a DMSO with DOX concentrations varying from 0 to 100 mg/L. The DOX loading level was calculated based on the following equation:

$$\text{Actual loading level (wt \%)} = \frac{\text{Mass of DOX extracted from micelles}}{\text{Mass of drug-loaded micelles initially used}} \times 100\%. \quad (1)$$

The particle size and zeta potential of the DOX-loaded peptide micelles were measured using dynamic light scattering (B1-200SM; Brookhaven Instrument., Holtsville, NY) equipped with a He–Ne laser beam at 658 nm (scattering angle: 90°) and Zetasizer (Masterizer 2000; Malvern Instrument, Worchestershire, UK), respectively. Briefly, the freeze-dried DOX-loaded micelles was dissolved in PBS buffer (20 mM) with pH values of 5.0, 6.0, 6.5, and 7.4. The particle size and zeta potential measurements were repeated for 30 runs for each sample, and the data were reported as the average of five readings.

The morphology of DOX-loaded peptide micelles was observed via field emission scanning electron microscopy (FE-SEM; JEOL JSM-7400F, Japan) and atomic force microscopy (AFM, Nanoscope IIIa AFM; Digital Instrument). Several droplets of DOX-loaded peptides micelles were added onto the silicon plate, and air-dried prior to SEM and AFM analysis. SEM was operated at an accelerating voltage of 6.0 kV in the transmission electron mode. The AFM was operated with the drive frequency of 330 $\pm$ 50 kHz and the voltage of 3.0–4.0 V. The drive amplitude was about 300 mV and the scan rate was 0.5–1.0 Hz.

Cytotoxicity test

The cytotoxity of DOX, micelles, and DOX-loaded micelles was studied against 4T1 cells, which are mammary tumor cells. Cells were maintained in RPMI 1640 supplemented with 10% FBS, 100 μg/mL penicillin and 100 units/mL streptomycin at 37°C, under the atmosphere of 5% CO_2. To assess the cytotoxicity of DOX, micelles, or DOX-loaded micelles in 4T1 cells, a standard methylthiazoltetrazolium (MTT) assay protocol was employed. Briefly, on a 96-well plate, cells were seeded at a density of 1×10^4 cells/well and allowed to grow for 24 h to reach 60–70% confluence. DOX, micelles, and DOX-loaded micelles solutions were prepared at stock concentrations. These solutions were diluted with growth media to give DOX and the micelles at various concentrations. Each well was replaced with 100 μL of pre-prepared growth medium-sample mixture. The cytotoxicity test was performed in replicates of eight wells. The plates were then returned to the incubator and maintained in 5% CO_2 at 37°C for 48 h. Upon replacing the wells with 100 μL of fresh medium and 20 μL of MTT solution (5 mg/mL in PBS buffer), the cells were incubated for another 4 h. Finally, the used media were removed and the internalized purple formazan crystals in each well were dissolved with 150 μL of DMSO. A 100 μL aliquot of the formazan solution was transferred from each well to a new 96-well plate, and the absorbance was measured using a microplate spectrophotometer (BioTek Instruments, Winooski, VT) at the wavelength of 550 and 690 nm. The absorbance readings of the formazan crystals were taken to be those at 550 nm subtracted by those at 690 nm. The results were expressed as a percentage of the absorbance of the blank.

In vitro DOX release study

The release profiles of DOX from micelles were studied using a dialysis bag (MWCO 1000 Da) at 37°C. To acquire sink conditions, drug release studies were performed at low drug concentrations. Briefly, 3 mg of DOX-loaded

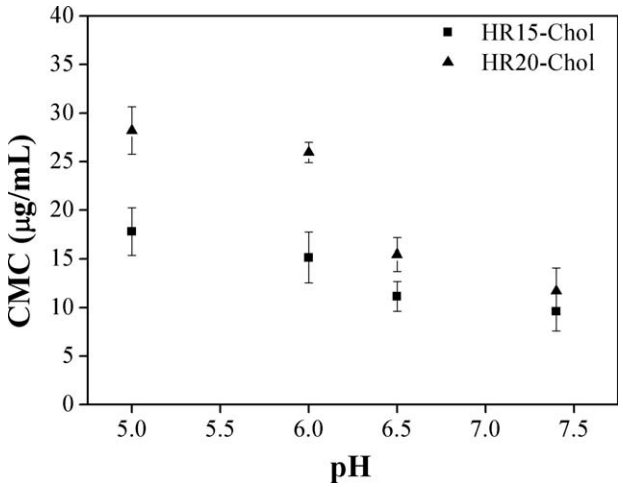

Figure 1. pH-Dependent CMC of micelles self-assembled from HR15-Chol and HR20-Chol.

freeze-dried micelles was dispersed in 3 mL of the respective PBS buffer and allowed to stabilize for 30 min before being placed in a dialysis bag. The dialysis bag was then immersed in 50 mL of PBS solution (pH 5.0, 6.0, 6.5, or 7.4) in a beaker. The beaker was then placed in a 37°C water bath and stirred at 100 rpm. The samples were drawn at desired time intervals and the drug concentration was analyzed using UV-vis spectrophotometry at 481 nm. The drug loading was calculated based on the standard curve obtained from DOX in the buffers. The in vitro release experiments were carried out in triplicate at each pH.

Results and Discussion

DOX-loaded micelle formation

To evaluate the pH-sensitivity of the micelles self-assembled from cholesterol conjugated peptides, CMCs was measured as a function of pH, as shown in Figure 1. The CMC values of the cholesterol conjugated peptides in PBS buffer (pH 5.0) were determined to be 17.8 and 28.2 μg/mL for HR15-Chol and HR20-Chol, respectively. The higher CMC value for HR20-Chol may be explained due to its longer hydrophilic segments. At pH 5.0, more histidine residues in HR20-Chol protonated as compared to HR15-Chol. Hence, with the same proportion of cholesterol moiety per conjugated peptide for both peptides, it required a greater driving force for micellar formation of HR20-Chol. Therefore, greater hydrophobic interaction was needed to counteract the greater electrostatic repulsive force from the hydrophilic blocks of HR20-Chol molecules when compared to HR15-Chol, leading to a higher CMC of HR20-Chol. For both peptides, the CMC values showed a decrease trend with the increase of pH values, especially from pH 6.0 to 6.5. The lowest CMC values were determined in PBS buffer with pH 7.4 (9.6 and 11.7 μg/mL for HR15-Chol and HR20-Chol, respectively). This decrease is due to the conversion of ionized histidine residues to hydrophobic ones by the protonation of imidazole groups.

Figure 2 shows the average hydrodynamic size and zeta potentials of blank and DOX-loaded micelles from both peptides at pH 5.0, 6.0, 6.5, and 7.4, respectively. The standard deviation bars were those between averages of multiple runs. Compared to blank micelles, the particle size of DOX-loaded HR15/20-Chol micelles shows a slightly increase due to the loading of DOX molecules in the core of micelles. It can also be seen from Figure 2A that the maximum size observed for DOX-loaded HR15-Chol and HR20-Chol was 187 nm (at pH 5.0) and 237 nm (at pH 5.0), respectively. For DOX-loaded HR15-Chol, the shorter histidine appeared to be responsible for the smaller size as compared to HR20-Chol. As the pH value increased to 7.4, the particle size of DOX-loaded HR15-Chol micelles decreased from 187 to 117 nm. For DOX-loaded HR20-Chol, the particle size showed the same trend (from 237 to 134 nm) with the increase of pH values. From Figure 2B, it can be observed that the zeta potential of DOX-loaded micelles is slightly lower than that of blank micelles. This can be explained that the larger particle size reduces the charge density of micelles. When the pH is 5.0, the histidine moieties may be

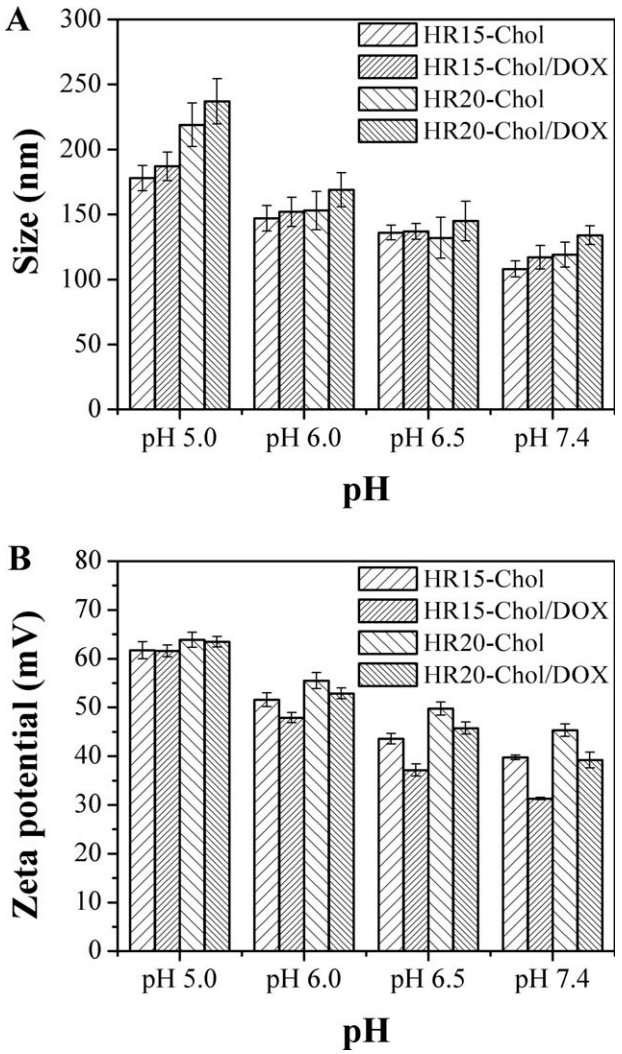

Figure 2. pH-Dependent (A) particle size and (B) zeta potential of blank and DOX-loaded micelles self-assembled from HR15-Chol and HR20-Chol.

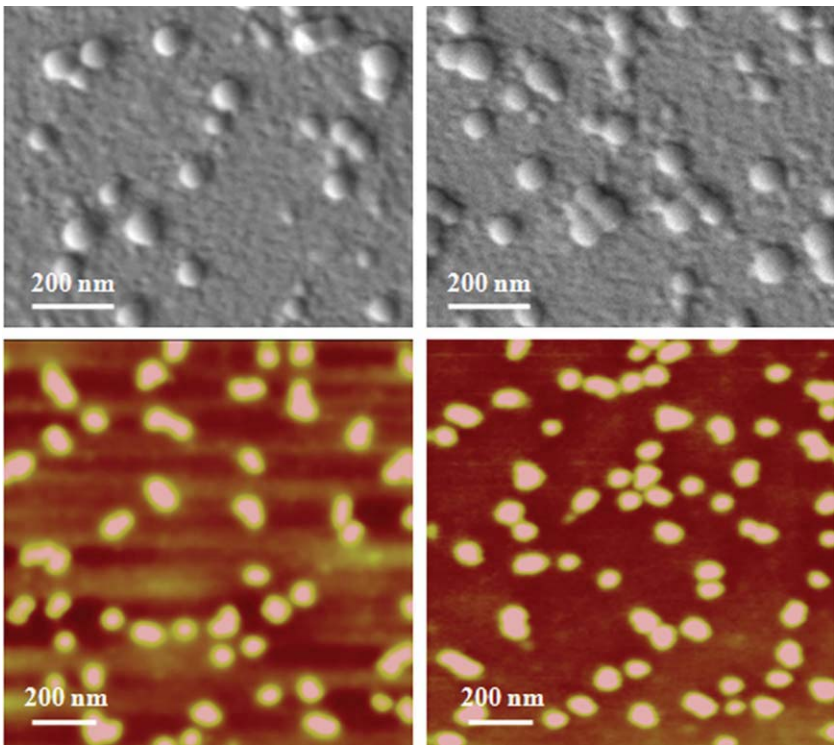

Figure 3. Typical SEM and AFM images of DOX-loaded micelles self-assembled from HR15-Chol and HR20-Chol.

[Color figure can be viewed in the online issue, which is available at www.interscience.wiley.com.]

more ionized, and thus the charge density of micelles surface increases. The increased electrostatic repulsion between histidine moieties induces the swelling of histidine residues. In addition, the conversion of nonionized histidine residues (at pH 7.4) to hydrophilic ones (at pH 5.0) by the protonation of imidazole groups could also induce the swelling of histidine residues, leading to the DOX-loaded micelles with bigger size. The highly charged character of micelles can prevent the aggregation of micelles and extend blood circulation times, which enable DOX-loaded micelles to accumulate in tumor or inflammation sites due to the enhanced permeation and retention effect. In addition, it can also increase the interactions between micelles and cell membranes, which can facilitate penetrating of cell membranes.

The formation of DOX-loaded micelles from both peptides (at pH 5.0) was further elucidated with the SEM and AFM images, as shown in Figure 3. The polydispersity in the size of micelles was around 0.28 from the dynamic light scattering (DLS) results. The micelles with smaller size are easier to penetrate the cell membranes. However, larger micelles could reduce higher drug loading efficiency. The particles ranged from 100 to 200 nm, which was smaller than that was determined by dynamic light scattering. This discrepancy could be due to shrinking of the particles during the drying process prior to SEM and AFM analysis. In addition, the DLS data presented an intensity average, which could also be another reason for the discrepancy between DLS and SEM data.

Coarse-grained simulations of micellization

To investigate the drug distribution inside the micelles and the pH sensitivity of cholesterol conjugated peptides, coarse-grained simulations were performed using dissipative particle dynamics method. This method was successfully applied in other drug delivery systems in our previous work.[40–42] The details of computation work are described in Supporting Information. Figure 4 shows the structure of DOX-loaded micelle and the structural transformation of blank micelles from pH $>$ 6.0 to pH $<$ 6.0. As can be observed from Figure 4A, cholesterol and histidine segments form the cores of micelles with hydrophilic arginine segments on the surface. DOX molecules are distributed mainly in the cholesterol layer due to the hydrophobic interaction between DOX and cholesterol molecules. The hydrophobic histidine layer can prevent the release of DOX at high pH values. However, the DOX molecules distributed in the histidine layer may be still release from the micelles even at high pH values, which may lead to the burst release. As shown in Figure 4B, at higher pH value than 6.0, due to the hydrophobic characters of cholesterol and histidine segments, the cholesterol conjugated peptides form core/shell micelles. Cholesterol and histidine segments form the cores of the micelles and are surrounded by arginine segments as a shell. When the pH value is decreased to lower than 6.0, the histidine residues are conversed to hydrophilic ones and trend to be swollen. This structural transformation of micelles can facilitate the release of DOX at lower pH conditions.

pH-dependent drug release

DOX was encapsulated into the micelles by membrane dialysis. The actual loading level of DOX in HR15-Chol and HR20-Chol micelles was about 9.8% and 12.3% by weight, respectively. In vitro drug release studies of the micelles

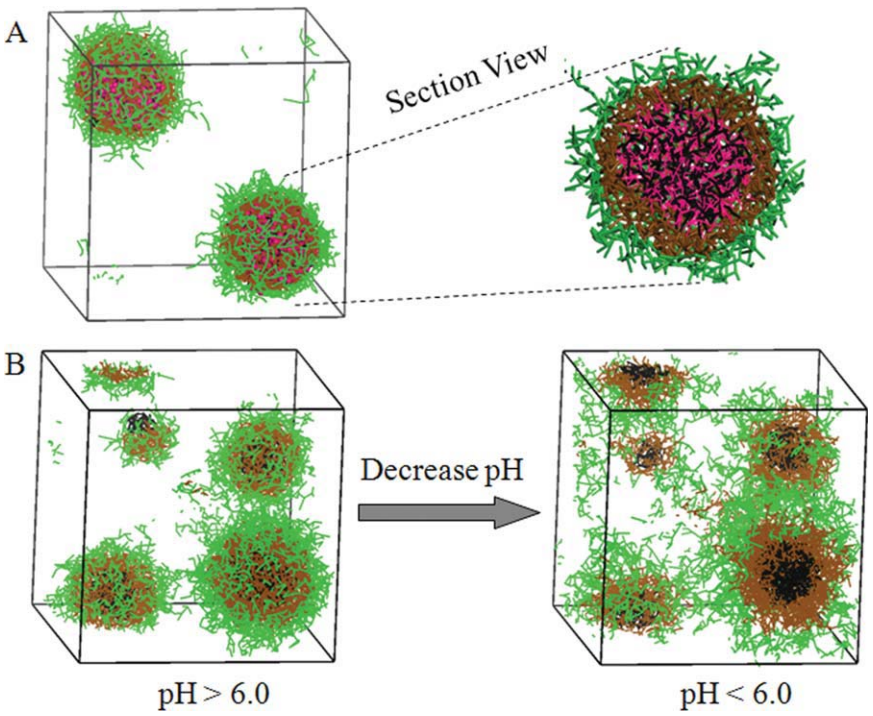

Figure 4. Typical simulated snapshots of (A) the structure of DOX-loaded micelle, and (B) the structural transformation of blank micelle from pH > 6.0 to pH < 6.0.

The red, green, brown, and black lines represent DOX, arginine, histidine, and cholesterol, respectively. Water is omitted. [Color figure can be viewed in the online issue, which is available at www.interscience.wiley.com.]

were performed under physiological conditions (PBS, pH 7.4) and in a slightly acidic environment (pH 5.0, pH 6.0, and pH 6.5) to simulate the pH of the endosomal and lysosomal microenvironments. Cholesterol conjugated peptides self-assemble into micelles which exhibit pH-dependent response characteristics. As we discussed above, the simulation results verified the transformation of micelle from dense to swollen conformation as the pH value decrease from pH $>$ 6.0 to pH $<$ 6.0. This structural transformation of micelles can facilitate the release of DOX at lower pH conditions. To rule out any effect of the dialysis process on the observed rate of release, the release of free DOX at 37°C with different pH buffer solutions was investigated as shown in Figure S3 (Supporting Information). It was observed that the release of free DOX is very fast at each pH conditions, and the release of DOX from micelles is pH dependent. The effect of the external pH on the drug-release rate from the micelles was shown in Figure 5. It can be observed that the release rate of DOX from the micelles is markedly influenced by pH values. At pH 7.4, the drug molecules can not release drastically from micelle due to the dense conformation of micelles. When the pH is lower (i.e., 6.5), the drug release rate is accelerated. In contrast, the drug release was much faster at pH 6.0 and 5.0. For both DOX-loaded micelles, the faster drug release rate in lower pH conditions could attribute to the looser micelle structure, which caused by the stronger protonation of imidazole groups in histidine residues at lower pH conditions. In addition, in lower pH medium, the histidine moieties may be more ionized, and thus the charge density of the micelle surface increases. The increased electrostatic repulsion between histidine moieties induces the swelling of histidine residues, which could also cause the looser micelle structure.

Furthermore, as can be seen in Figure S3 (Supporting Information), it was obvious that the drug release rates were delayed with increasing the histidine length at four pH conditions, especially at the early release time (i.e., the first 10 h). The longer histidine length may increase the drug diffuse distance, which may delay DOX molecules diffuse from the core of micelles to external medium.

Release mechanism studies

The drug release from a polymeric matrix is a very complicated process. Several mechanisms, such as diffusion of the drug molecules and erosion of the polymer matrix, may be responsible for the overall release of a drug from a polymeric matrix. To investigate the nature of drug release behaviors with different mechanisms and various geometries, a classic empirical exponential expression was established by Ritger and Peppas [43]

$$\frac{M_t}{M_\infty} = kt^n, \tag{2}$$

$$\log\left(\frac{M_t}{M_\infty}\right) = n\log t + \log k, \tag{3}$$

where M_t and M_∞ are the absolute cumulative amount of drug released at time t and infinite time, respectively, k is a constant incorporating structural and geometric characteristics of the device, and n is the release exponent, indicative of the

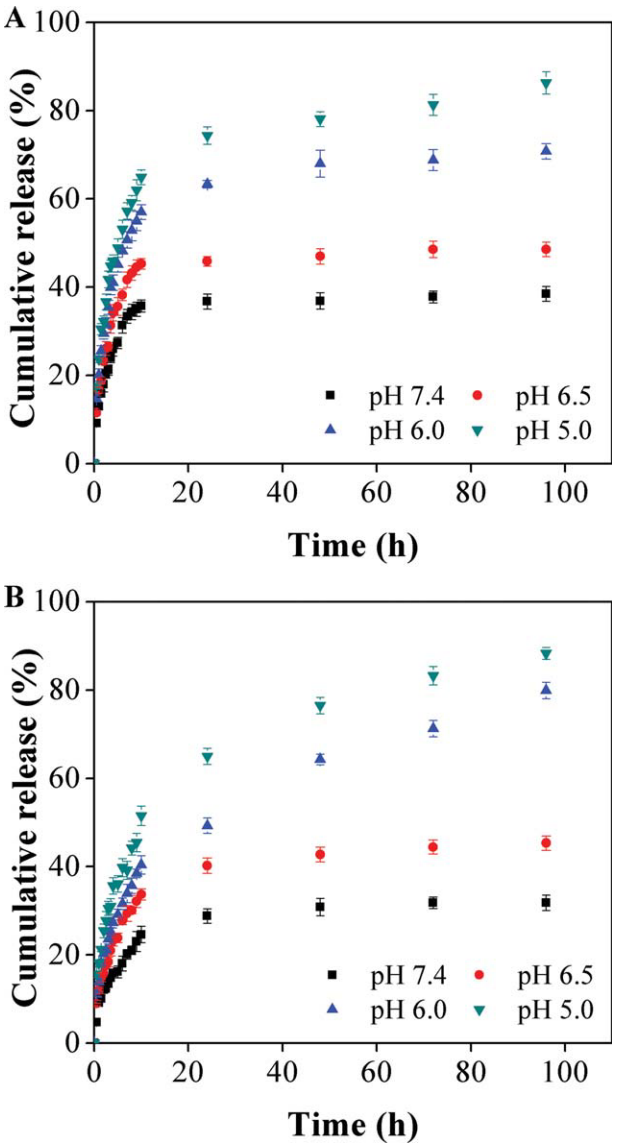

Figure 5. In vitro drug release profiles from DOX-loaded micelles self-assembled from (A) HR15-Chol and (B) HR20-Chol at pH 7.4, 6.5, 6.0, and 5.0 PBS solutions at 37°C.

[Color figure can be viewed in the online issue, which is available at www.interscience.wiley.com.]

mechanism of drug release. The power law equation can be observed as the superposition of two processes of Fickian diffusion and case-II transport (swelling-controlled drug release). If Fickian diffusion occurs, n equals 0.43 for spheres. When swelling-controlled drug release dominates, the n value is 0.85 for spheres.[43,44]

Figure 6 shows a typical plot of log (M_t/M_∞) against log (t) for DOX release from peptides micelles at various pH values. The fitting data, including the release exponent n, rate constant of k, and the correlation coefficient R^2 from peptides micelles at 37°C are shown in Table 1. The release of DOX for both types of micelles was divided into two stages, one is from 0 to 10 h, and the other is from 10 to 96 h. For HR15-Chol/DOX systems, good linearity can be observed for the first 10 h (Figure 6A). The n values at different pH conditions are very close to 0.45, indicating that the DOX release behavior in the first 10 h at different pH values corresponds to the Fickian diffusion model. The k values for HR15-Chol/DOX systems increase when pH is decreased, indicating that the release rate of DOX increase with decreasing pH values. This could attribute to the transformation of histidine residues from hydrophobic to hydrophilic ones as pH decreases, facilitating the release of DOX molecules. For the second stage, the n values are 0.10, 0.08, 0.05, and 0.03 at pH 5.0, 6.0, 65, and 7.4, respectively, which are much lower than 0.43. The empirical approximation does not apply to this period of release any more. For HR20-Chol/DOX systems, good linearity can be observed for the first 10 h (Figure 6B). The n values are also very close to 0.45, indicating that the DOX release behavior from HR20-Chol micelles at different pH values in the first 10 h also corresponds to the Fickian diffusion model. The k values for HR20-Chol/DOX systems show an increasing trend with decreasing pH values, indicating that the release rate of

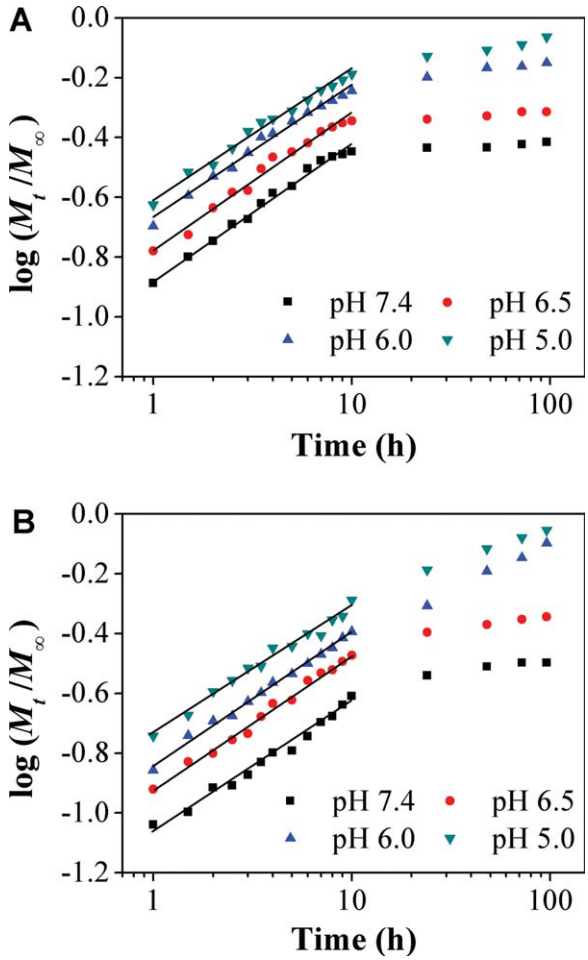

Figure 6. Plots of log (M_t/M_∞) against log (t) for DOX release from micelles self-assembled from (A) HR15-Chol and (B) HR20-Chol at various pH values, T = 37°C.

[Color figure can be viewed in the online issue, which is available at www.interscience.wiley.com.]

Table 1. Release Exponent (n), Rate Constant (k), and Correlation Coefficient (R^2) for HR15-Chol and HR20-Chol Micelles at Different pH Values; $T = 37°C$

Matrix	pH	n (0–10 h)	k (0–10 h)	R^2 (0–10 h)	n (10–96 h)	R^2 (10–96 h)
HR15-Chol	5.0	0.42	24.9	0.988	0.10	0.976
	6.0	0.45	21.3	0.987	0.08	0.984
	6.5	0.46	16.7	0.982	0.05	0.985
	7.4	0.46	13.2	0.990	0.03	0.980
HR20-Chol	5.0	0.42	18.5	0.983	0.22	0.997
	6.0	0.44	14.5	0.994	0.34	0.998
	6.5	0.45	11.9	0.991	0.09	0.992
	7.4	0.43	8.67	0.983	0.08	0.959

DOX increase with decreasing pH values. At higher pH value (i.e., pH 7.4), the hydrophobic histidine layer can prevent the release of DOX. However, at lower pH value (i.e., pH 5.0), histidine residues are conversed to hydrophilic ones which can facilitate the release of DOX. At the same pH values (i.e., pH 7.4, 6.5, 6.0, and 5.0), HR20-Chol/DOX systems have smaller rate constant (i.e., k) values as compared to HR15-Chol/DOX systems, indicating that DOX-loaded HR20-Chol micelles have lower release rates in the first 10 h. This can be explained that the longer histidine residues have stronger capability of preventing DOX release from micelles, leading to a more sustained release for HR20-Chol/DOX systems. For the second stage, the n values are also much lower than 0.43. The DOX release behavior in this stage can also not be analyzed using the empirical approximation equation.

As an overall result, pH value and histidine residue length play an important role in DOX release process. The drug release rates were significantly accelerated when pH of the solution changed from 7.4 to 5.0. At lower pH values (e.g. pH 6.0 and 5.0), the imidazole side group in histidine is protonated. This formation of hydrophilic ionized histidine residues was benefit for the release of DOX, leading to a faster release at lower pH conditions.

Cytotoxicity of DOX-loaded micelles

Cytotoxic effects of cholesterol conjugated peptides, free DOX, DOX-loaded HR15-Chol, and HR20-Chol micelles were studied against 4T1 cells by MTT assay, as shown in Figure 7. The cytotoxicity of HR15-Chol and HR20-Chol increased slightly with increasing the concentration of peptides (Figure 7A). The percentage of viable cells for HR15-Chol and HR20-Chol especially at their highest concentration (i.e., 400 μg/mL) was about 88.9% and 83.6%, respectively. No obvious cytotoxicity of blank HR15-Chol/HR20-Chol micelles was observed in 4T1 cells. The cytotoxicity of free DOX and DOX-loaded peptides micelles is shown in Figure 7B. The IC50 value of DOX, a concentration at which 50% cells are killed, was 2.58, 3.82, and 6.17 μg/mL for free DOX, DOX-loaded micelles from HR15-Chol and HR20-Chol against 4T1 cells, respectively. The cytotoxicity of DOX-loaded micelles was lower than free DOX against 4T1 cells. This would be because the DOX release from micelles might be a slow process and DOX-loaded micelles might not enter the nucleus as quickly as the free DOX. It is also observed that DOX-loaded HR15-Chol micelles showed a little higher cytotoxicity than DOX-loaded HR20-Chol micelles. This result may be attributed to the faster DOX release from the HR15-Chol micelles as compared to HR20-Chol micelles. In addition, when the DOX concentration increased to 10 μg/mL, the cell viability for DOX loaded HR15-Chol and HR20-Chol micelles was 7.87% and

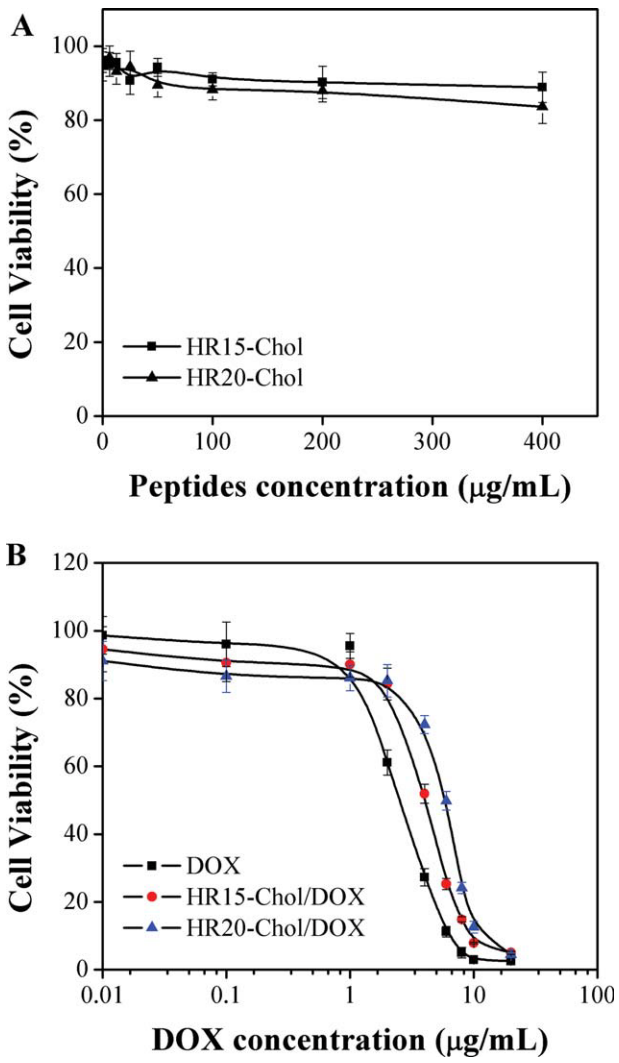

Figure 7. The cytotoxicity of (A) cholesterol conjugated peptides micelles at the concentrations specified and (B) free DOX and DOX-loaded micelles in 4T1 cells at the DOX concentrations specified.

[Color figure can be viewed in the online issue, which is available at www.interscience.wiley.com.]

12.60%, respectively, indicating that the DOX-loaded peptide micelles could also kill the cells efficiently.

Conclusions

In this study, pH-sensitive micelles self-assembled from amphiphilic cholesterol conjugated HR15 and HR20 polypeptides were developed for DOX delivery. The low CMC values of these peptides can markedly improve micellar stability and extend the range of applications of micelles in controlled drug delivery. The hydrophobic core (i.e., cholesterol) is highly compatible with cell membranes. The hydrophilic shell is arginine which is a cell penetrating residue. And the DOX release rate is controlled by histidine layer. The release of DOX from the micelles is significantly accelerated by decreasing pH from 7.4 to 5.0 which just fits the pathological process. From the coarse-grained simulations, DOX molecules distribute inside the core of micelles. The simulation results also illuminate that the histidine layer shows a transformation from dense to swollen conformation as the pH decrease from pH $>$ 6.0 to pH $<$ 6.0. The drug release profiles at different pH values are well fitted by a classical empirical power law. According to the release exponent n and rate constant k, the release of DOX in the first 10 h follows the Fickian diffusion and DOX has a faster release at lower pH conditions. All these characteristics demonstrated that this system has potential applications in cancer drug delivery.

Acknowledgments

This work was financially supported by National Natural Science Foundation of China (No. 20536020 and No. 20776049) and Guangdong Province Science Foundation (No. 9251064101000009). The first author also appreciates the China Scholarship Council's support for his visiting study at IBN.

Literature Cited

1. Bae Y, Kataoka K. Intelligent polymeric micelles from functional poly(ethylene glycol)-poly(amino acid) block copolymers. *Adv Drug Deliv Rev*. 2009;61:768–784.
2. Bromberg L. Polymeric micelles in oral chemotherapy. *J Control Release*. 2008;128:99–112.
3. Kretlow JD, Mikos AG. From material to tissue: biomaterial development, scaffold fabrication, and tissue engineering. *AIChE J*. 2008; 54:3048–3067.
4. Kryscio DR, Peppas NA. Mimicking biological delivery through feedback-controlled drug release systems based on molecular imprinting. *AIChE J*. 2009;55:1311–1324.
5. Husseini GA, Pitt WG. Micelles and nanoparticles for ultrasonic drug and gene delivery. *Adv Drug Deliv Rev*. 2008;60:1137–1152.
6. Oh KT, Lee ES, Kim D, Bae YH. L-Histidine-based pH-sensitive anticancer drug carrier micelle: reconstitution and brief evaluation of its systemic toxicity. *Int J Pharm*. 2008;358:177–183.
7. Smart T, Lomas H, Massignani M, Flores-Merino MV, Perez LR, Battaglia G. Block copolymer nanostructures. *Nano Today*. 2008; 3:38–46.
8. Ganta S, Devalapally H, Shahiwala A, Amiji M. A review of stimuli-responsive nanocarriers for drug and gene delivery. *J Control Release*. 2008;126:187–204.
9. Peer D, Karp JM, Hong S, FaroKhzad OC, Margalit R, Langer R. Nanocarriers as an emerging platform for cancer therapy. *Nat Nanotechnol*. 2007;2:751–760.
10. Mitragotri S, Lahann J. Physical approaches to biomaterial design. *Nat Mater*. 2009;8:15–23.
11. Feng SS, Zhao LY, Zhang ZP, Bhakta G, Win KY, Dong YC, Chien S. Chemotherapeutic engineering: vitamin E TPGS-emulsified nanoparticles of biodegradable polymers realized sustainable paclitaxel chemotherapy for 168 h in vivo. *Chem Eng Sci*. 2007;62:6641–6648.
12. Sarker DK. Engineering of nanoemulsions for drug delivery. *Curr Drug Deliv*. 2005;2:297–310.
13. Shen Y, Zhan Y, Tang J, Xu P, Johnson PA, Radosz M. Multifunctioning pH-responsive nanoparticles from hierarchical self-assembly of polymer brush for cancer drug delivery. *AIChE J*. 2008;54:2979–2989.
14. Kim D, Lee ES, Oh KT, Gao ZG, Bae YH. Doxorubicin-loaded polymeric micelle overcomes multidrug resistance of cancer by double-targeting folate receptor and early endosomal pH *Small*. 2008; 4:2043–2050.
15. Hrubý M, Koňák C, Ulbrich K. Polymeric micellar pH-sensitive drug delivery system for doxorubicin. *J Control Release*. 2005; 103:137–148.
16. Wei L, Cai C, Lin J, Chen T. Dual-drug delivery system based on hydrogel/micelle composites. *Biomaterials*. 2009;30:2606–2613.
17. Xianzheng Z, Hua W, Cheng C, Cheng SX, Zhuo RX. Self-assembled, thermosensitive micelles of a star block copolymer based on PMMA and PNIPAAm for controlled drug delivery. *Biomaterials*. 2007;28:99–107.
18. Li YY, Zhang XZ, Cheng H, Kim GC, Cheng SX, Zhuo RX. Novel stimuli-responsive micelle self-assembled from Y-shaped P(UA-Y-NIPAAm) copolymer for drug delivery. *Biomacromolecules*. 2006; 7:2956–2960.
19. Collet E, Lemée-Cailleau M-H, Cointe MB-L, Cailleau H, Wulff M, Luty T, Koshihara S-Y, Meyer M, Toupet L, Rabiller P, Techert S. Micellar nanocontainers distribute to defined cytoplasmic organelles. *Science*. 2003;300:615–618.
20. Fernandez-Carneado J, Kogan MJ, Castel S, Giralt E. Potential peptide carriers: amphipathic proline-rich peptides derived from the n-terminal domain of gamma-zein. *Angew Chem Int Ed Engl*. 2004; 43:1811–1814.
21. Qiu LY, Bae YH. Self-assembled polyethylenimine-graft-poly(ε-caprolactone) micelles as potential dual carriers of genes and anticancer drugs. *Biomaterials*. 2007;28:4132–4142.
22. Lin J, Zhu J, Chen T, Lin S, Cai C, Zhang L, Zhuang Y, Wang X-S. Drug releasing behavior of hybrid micelles containing polypeptide triblock copolymer. *Biomaterials*. 2008;30:108–117.
23. Yin H, Bae YH. Physicochemical aspects of doxorubicin-loaded pH-sensitive polymeric micelle formulations from mixtures of poly(L-histidine)-b-poly(ethylene glycol)/ poly(L-lactide)-b-poly(ethylene glycol). *Eur J Pharm Biopharm*. 2008;71:223–230.
24. Schramm OG, Meier MAR, Hoogenboom R, van Erp HP, Gohy J-F, Schubert US. Polymeric nanocontainers with high loading capacity of hydrophobic drugs. *Soft Matter*. 2009;5:1662–1667.
25. Langer R, Peppas NA. Advances in biomaterials, drug delivery, and bionanotechnology. *AIChE J*. 2003;49:2990–3006.
26. Geng Y, Dalhaimer P, Cai SS, Tsai R, Tewari M, Minko T, Discher DE. Shape effects of filaments versus spherical particles in flow and drug delivery. *Nat Nanotechnol*. 2007;2:249–255.
27. Miao ZM, Cheng SX, Zhang XZ, Zhuo RX. Study on drug release behaviors of poly-alpha,beta-[N-(2-hydroxyethyl)-L-aspartamide]-g-poly(epsilon-caprol actone) nano- and microparticles. *Biomacromolecules*. 2006;7:2020–2026.
28. Biggs S, Sakai K, Addison T, Schmid A, Armes SP, Vamvakaki M, Butun V, Webber G. Layer-by-layer formation of smart particle coatings using oppositely charged block copolymer micelles. *Adv Mater*. 2007;19:247–250.
29. Engin K, Leeper DB, Cater JR, Thistlethwaite AJ, Tupchong L, McFarlane JD. Extracellular pH distribution in human tumours. *Int J Hyperthermia*. 1995;11:211–216.
30. Schmid S, Fuchs R, Kielian M, Helenius A, Mellman I. Acidification of endosome subpopulations in wild-type Chinese-hamster over cells and temperature-sensitive acidification-defective mutants. *J Cell Biol*. 1989;108:1291–1300.
31. Schmid SL, Fuchs R, Male P, Mellman I. Two distinct subpopulations of endosomes involved in membrane recycling and transport to lysosomes. *Cell*. 1988;52:73–83.
32. Turk MJ, Reddy JA, Chmielewski JA, Low PS. Characterization of a novel pH-sensitive peptide that enhances drug release from folate-targeted liposomes at endosomal pHs. *Biochim Biophys Acta*. 2002;1559:56–68.
33. Rothbard JB, Garlington S, Lin Q, Kirschberg T, Kreider E, McGrane PL, Wender PA, Khavari PA. Conjugation of arginine

oligomers to cyclosporin A facilitates topical delivery and inhibition of inflammation. *Nat Med*. 2000;6:1253–1257.
34. Nori A, Jensen KD, Tijerina M, Kopeckova P, Kopecek J. Tat-conjugated synthetic macromolecules facilitate cytoplasmic drug delivery to human ovarian carcinoma cells. *Bioconjug Chem*. 2003;14:44–50.
35. Christie RJ, Grainger DW. Design strategies to improve soluble macromolecular delivery constructs. *Adv Drug Deliv Rev*. 2003;55: 421–437.
36. Yu W, Pirollo KF, Yu B, Rait A, Xiang LM, Huang WQ, Zhou Q, Ertem G, Chang EH. Enhanced transfection efficiency of a systemically delivered tumor-targeting immunolipoplex by inclusion of a pH-sensitive histidylated oligolysine peptide. *Nucleic Acids Res*. 2004;32:e48.
37. Aoki Y, Hosaka S, Kawa S, Kiyosawa K. Potential tumor-targeting peptide vector of histidylated oligolysine conjugated to a tumor-homing RGD motif. *Cancer Gene Ther*. 2001;8:783–787.
38. Ikonen E. Cellular cholesterol trafficking and compartmentalization. *Nat Rev Mol Cell Biol*. 2008;9:125–138.
39. Mann A, Thakur G, Shukla V, Ganguli M. Peptides in DNA delivery: current insights and future directions. *Drug Discov Today*. 2008;13:152–160.
40. Guo XD, Zhang LJ, Qian Y, Zhou J. Effect of composition on the formation of poly(DL-lactide) microspheres for drug delivery systems: mesoscale simulations. *Chem Eng J*. 2007;131:195–201.
41. Guo XD, Tan JPK, Zhang LJ, Khan M, Liu SQ, Yang YY, Qian Y. Phase behavior study of paclitaxel loaded amphiphilic copolymer in two solvents by dissipative particle dynamics simulations. *Chem Phys Lett*. 2009;473:336–342.
42. Guo XD, Tan JPK, Kim SH, Zhang LJ, Zhang Y, Hedrick JL, Yang YY, Qian Y. Computational studies on self-assembled paclitaxel structures: templates for hierarchical block copolymer assemblies and sustained drug release. *Biomaterials*. 2009;30:6556–6563.
43. Ritger PL, Peppas NA. A simple equation for description of solute release I. Fickian and non-Fickian release from non-swellable devices in the form of slabs, spheres, cylinders or discs. *J Control Release*. 1987;5:23–36.
44. Siepmann J, Gopferich A. Mathematical modeling of bioerodible, polymeric drug delivery systems. *Adv Drug Deliver Rev*. 2001;48: 229–247.

Manuscript received Aug. 10, 2009, and revision received Sept. 29, 2009.